Self-diffusion of biomolecules in solution

Michio Tokuyama,[1] Tatsuo Moriki,[2] and Yuto Kimura[2]
[1]*World Premier International Research Center, Advanced Institute for Materials Research and Institute of Fluid Science, Tohoku University, Sendai 980-8577, Japan*
[2]*Department of Nanomechanics Engineering, Tohoku University, Sendai 980-8579, Japan*
(Received 25 January 2011; published 16 May 2011)

A simple soft-core model potential is proposed to discuss the self-diffusion of biomolecules in solution. Extensive Brownian-dynamics simulations are performed to obtain the long-time self-diffusion coefficient. Then the simulation results are compared with the experimental data from a unified point of view recently obtained for suspensions of hard spheres. Thus, it is shown that the proposed potential can qualitatively well describe the experimental data.

DOI: 10.1103/PhysRevE.83.051402 PACS number(s): 83.80.Hj, 87.15.Vv, 05.40.−a, 64.70.pv

I. INTRODUCTION

The main purpose of the present paper is to propose a simple soft-core model potential to describe the self-diffusion of biomolecules in solution. Self-diffusion of hard-sphere colloids has been studied experimentally [1–6], theoretically [7–12], and numerically [13,14] over the last two decades because of their simple nature. Self-diffusion of protein molecules in solution is also an interesting subject for studying a variety of biological phenomena [15–27]. Until now, however, its theoretical understanding is still incomplete. This is mainly for the following two reasons. The first is that the conventional soft-core potential $U_n(r)$ is not appropriate to describe biomolecules as soft particles; it is given by

$$U_n(r) = k_B T \left(\frac{\sigma}{r}\right)^n, \tag{1}$$

where n is an integer, T temperature, and σ a positive constant. In Eq. (1), the effective diameter σ_{eff} is determined by $U_n(\sigma_{eff}) = k_B T$. Hence $\sigma_{eff} = \sigma$ here. In fact, for any system in which the volume fraction ϕ $(= \pi\sigma^3 N/6V)$ is a control parameter, the long-time self-diffusion coefficients obtained by experiments and simulations for suspensions are well described by a singular function of ϕ as [28]

$$D_S^L(\phi) = \frac{D_S^S(\phi)}{1 + \kappa \frac{D_S^S(\phi)}{D_0} \left(\frac{\phi}{\phi_c}\right)\left(1 - \frac{\phi}{\phi_c}\right)^{-2}} \tag{2}$$

with the coefficient [29]

$$\kappa = \int_1^\infty d\hat{r}\hat{r}^3 \left(-\frac{\partial \hat{U}_n(r)}{\partial \hat{r}}\right) = \frac{n}{n-3}, \tag{3}$$

where D_S^S denotes the short-time self-diffusion coefficient, ϕ_c a fictive singular point to be determined by fitting, $\hat{r} = r/\sigma$, and $\hat{U}_n = U_n/k_B T$. Here m is the particle mass, N the total number of particles, V the total volume of the system, and D_0 a single-particle diffusion constant. As discussed in a previous paper [30], the analyses of several sets of experimental data for biomolecules by Eq. (2) suggest that their short-time behavior is hard-sphere-like because D_S^S is described well by the relation obtained for a suspension of hard spheres by Tokuyama and Oppenheim [11]. Those analyses also suggest that the long-time behavior is soft-sphere-like because κ is found to be 2.0 but not 1.0. From Eq. (3), this leads to $n = 6$. Then Brownian-dynamics (BD) and molecular-dynamics (MD) simulations were performed with the conventional soft-core potential given by Eq. (1) with $n = 6$. As is shown later, however, both simulation results suggest that the potential given by Eq. (1) cannot describe the experimental data qualitatively or quantitatively. This must be because that potential has no effective core. Hence we propose a modified soft-core potential with an effective core as

$$U_n(r) = k_B T \left(\frac{\sigma}{r - b\sigma}\right)^n, \tag{4}$$

where b is a positive constant to be determined. Here $\sigma_{eff} = (1 + b)\sigma$. Hence the volume fraction ϕ is given by $\phi = (\pi\sigma^3 N/6V)(1 + b)^3$. In order to use Eq. (2), therefore, one might replace ϕ by $\phi/(1 + b)^3$. The constant b is chosen so that the BD simulation results for D_S^L coincide with those of MD when the values of D_S^S are taken from the theoretical values for hard spheres. Thus, one finds $b = 0.25$.

The second reason for the lack of theoretical understanding is that the hydrodynamic interactions between biomolecules cannot be calculated analytically and numerically. There are two kinds of hydrodynamic interaction. One is a short-time hydrodynamic interaction, which leads to a short-time self-diffusion coefficient D_S^S. The other is a long-time hydrodynamic interaction, which leads to a long-time self-diffusion coefficient D_S^L. Both interactions have been analytically calculated only for hard spheres [11].

In Sec. II, we first derive the starting stochastic equations for the position vectors of particles from the generalized nonlinear Langevin equations for many particles. We then perform BD simulations based on those equations. In Sec. III, we briefly review the formal expressions for the long-time self-diffusion coefficient D_S^L both in suspensions and in molecular systems from first principles. We then discuss the important role of the two kinds of hydrodynamic interaction in self-diffusion by comparing the experimental data and the simulation results for hard-sphere colloids. In Sec. IV, we discuss two types of hydrodynamic effect on the self-diffusion coefficient in hard-sphere suspensions, the short- and the long-time effects. In Sec. V, we analyze the experimental data for biomolecules by using Eq. (2) and show that they can be described well at $\kappa = 2$ if the theoretical values for a suspension of hard spheres are taken as D_S^S. In Sec. VI, we perform BD simulations to obtain

the long-time self-diffusion coefficients for biomolecules. In order to find a reasonable value of b, we also perform MD simulations. Comparing both simulation results, we then find $b = 0.25$. Thus, the BD simulation results are compared with experimental data and are shown to be in good agreement with them qualitatively. In Sec. VII, we conclude with a summary.

II. STARTING EQUATION

In the following, we assume that the short-time hydrodynamic interactions between soft spheres behave in the same manner as those in hard spheres with diameter σ. As is shown later, this is true for the modified potential. We consider a suspension of N identical particles with mass m and diameter σ in the total volume V at temperature T and volume fraction ϕ $(= \pi\sigma^3 N/6V)$. Let $\{\boldsymbol{X}(t), \boldsymbol{P}(t)\} = \{\boldsymbol{X}_i(t), \boldsymbol{P}_i(t);\ i = 1, \ldots, N\}$ denote a set of variables, where $\boldsymbol{X}_i(t)$ and $\boldsymbol{P}_i(t)$ denote the position vector and the momentum of the ith particle, respectively. It is also convenient to introduce a generating function for $\{\boldsymbol{X}, \boldsymbol{P}\}$ to have a set of values $\{\boldsymbol{x}, \boldsymbol{p}\}$ by $\Pi_{\boldsymbol{x},\boldsymbol{p}}(t) = \prod_{i=1}^{N} \delta(\boldsymbol{X}_i(t) - \boldsymbol{x}_i)\delta(\boldsymbol{P}_i(t) - \boldsymbol{p}_i)$. Then, one can derive the nonlinear Langevin equation for $\boldsymbol{P}_i(t)$, on a time scale of order t_B [11,12],

$$\frac{d}{dt}\boldsymbol{P}_i(t) = -\frac{1}{m}\sum_{j=1}^{N} \boldsymbol{\zeta}_{ij}(\boldsymbol{X}(t)) \cdot \boldsymbol{P}_j(t) + \boldsymbol{F}_i(t) + \boldsymbol{R}_i(t), \tag{5}$$

and its corresponding stochastic Fokker-Planck equation [32]

$$\frac{\partial}{\partial t}\Pi_{\boldsymbol{x}\boldsymbol{p}}(t) = \Omega(\boldsymbol{x}, \boldsymbol{p})\Pi_{\boldsymbol{x}\boldsymbol{p}}(t) + \xi_{\boldsymbol{x}\boldsymbol{p}}(t) \tag{6}$$

with the Fokker-Planck operator

$$\Omega(\boldsymbol{x}, \boldsymbol{p}) = -\sum_{i=1}^{N}\left[\frac{\boldsymbol{p}_i}{m}\cdot\frac{\partial}{\partial \boldsymbol{x}_i} + \frac{\partial}{\partial \boldsymbol{p}_i}\cdot\boldsymbol{F}_i\right] + \sum_{i=1}^{N}\sum_{j=1}^{N}\frac{\partial}{\partial \boldsymbol{p}_i}\cdot\boldsymbol{\zeta}_{ij}\cdot\left[\frac{1}{m}\boldsymbol{p}_j + k_B T\frac{\partial}{\partial \boldsymbol{p}_j}\right], \tag{7}$$

where the function $\xi_{\boldsymbol{x}\boldsymbol{p}}(t)$ denotes a Gaussian, Markov noise with zero mean and satisfies

$$\langle \xi_{\boldsymbol{x}\boldsymbol{p}}(t)\xi_{\boldsymbol{x}'\boldsymbol{p}'}(0)\rangle = 2k_B T\delta(t)\sum_{i=1}^{N}\sum_{j=1}^{N}\frac{\partial}{\partial \boldsymbol{p}_i}\cdot\boldsymbol{\zeta}_{ij}\cdot\frac{\partial}{\partial \boldsymbol{p}'_j} \times \delta(\boldsymbol{x} - \boldsymbol{x}')\delta(\boldsymbol{p} - \boldsymbol{p}')w(\boldsymbol{x}, \boldsymbol{p}). \tag{8}$$

Here $w(\boldsymbol{x}, \boldsymbol{p})$ $(= \langle\Pi_{\boldsymbol{x}\boldsymbol{p}}(0)\rangle)$ denotes the equilibrium distribution function which satisfies $\Omega w = 0$, the brackets $\langle\cdots\rangle$ the average over an equilibrium ensemble, and t_B $(= m/\zeta_0)$ a Brownian relaxation time, where ζ_0 is a single-particle friction constant. The random force $\boldsymbol{R}_i(t)$ is given by

$$\boldsymbol{R}_i(t) = \int\int d\boldsymbol{x}d\boldsymbol{p}\,\boldsymbol{p}_i\xi_{\boldsymbol{x}\boldsymbol{p}}(t), \tag{9}$$

and satisfies

$$\langle \boldsymbol{R}_i(t)\rangle = 0, \quad \langle \boldsymbol{R}_i(t)\boldsymbol{R}_j(t')\rangle = 2k_B T\langle\boldsymbol{\zeta}_{ij}\rangle\delta(t - t'). \tag{10}$$

The friction tensor $\boldsymbol{\zeta}_{ij}$ is given by

$$\boldsymbol{\zeta}_{ij} = \zeta_0[(\mathbf{1} + \boldsymbol{g})^{-1}]_{ij}, \tag{11}$$

where the tensor $\boldsymbol{g}_{ij}$ indicates the hydrodynamic interaction between particles i and j (see Ref. [11] for details), and $\boldsymbol{g}_{ii} = \mathbf{0}$. The function $\boldsymbol{F}_i$ denotes a total force acting on the ith particle from the others and is given by

$$\boldsymbol{F}_i(t) = -\frac{\partial}{\partial \boldsymbol{X}_i}\sum_{j\neq i} U_n(|\boldsymbol{X}_i - \boldsymbol{X}_j|). \tag{12}$$

In order to distinguish the short-time hydrodynamic interactions from the long-time ones, we next introduce a projection operator $\wp$ by

$$\wp G = \left.\frac{\langle G\Pi_{\boldsymbol{p}}(0)\rangle}{\langle\Pi_{\boldsymbol{p}}(0)\rangle}\right|_{\boldsymbol{p}=\boldsymbol{P}(0)}, \tag{13}$$

where $\Pi_{\boldsymbol{p}}(t) = \int d\boldsymbol{x}\Pi_{\boldsymbol{x}\boldsymbol{p}}(t)$ and G is an arbitrary function. Then, use of Eqs. (5) and (6) leads to

$$\frac{d}{dt}\boldsymbol{P}_i(t) = e^{t\hat{\Omega}(\boldsymbol{X},\boldsymbol{P})}(\wp + Q)\hat{\Omega}\boldsymbol{P}_i(0) + \boldsymbol{R}_i(t) \tag{14}$$

$$= -\frac{\langle\boldsymbol{\zeta}_{ii}\rangle}{m}\cdot\boldsymbol{P}_i(t) + \boldsymbol{F}_i(t) + \boldsymbol{R}_i(t) + \boldsymbol{H}_i(t) \tag{15}$$

with the term due to the long-time hydrodynamic interactions

$$\boldsymbol{H}_i(t) = \frac{-1}{m}\sum_{j=1}^{N} e^{t\hat{\Omega}(\boldsymbol{X},\boldsymbol{P})}[\zeta_{ij}(\boldsymbol{X}) - \delta_{ij}\langle\boldsymbol{\zeta}_{ij}\rangle]\cdot\boldsymbol{P}_j(0), \tag{16}$$

where $\hat{\Omega}(\boldsymbol{x}, \boldsymbol{p})\delta(\boldsymbol{x} - \boldsymbol{x}')\delta(\boldsymbol{p} - \boldsymbol{p}') = \Omega(\boldsymbol{x}', \boldsymbol{p}')\delta(\boldsymbol{x} - \boldsymbol{x}')\delta(\boldsymbol{p} - \boldsymbol{p}')$ and $Q = 1 - \wp$. The first term in Eq. (15) can be written as [32,34]

$$\langle\boldsymbol{\zeta}_{ii}\rangle = \zeta_0[1 + L(\phi)]\mathbf{1}, \tag{17}$$

where $L(\phi)$ indicates the term due to the short-time hydrodynamic interactions. In the following, we neglect the term $H_i(t)$ because its numerical calculation is still not possible. On the time scale of order t_D $(= \sigma^2/D_0)$, one can safely neglect the inertia term of Eq. (15), where $D_0 = k_B T/\zeta_0$. Thus, one obtains

$$\frac{d}{dt}\boldsymbol{X}_i(t) = D_S^S(\phi)\frac{\boldsymbol{F}_i(t)}{k_B T} + \boldsymbol{f}_i(t), \tag{18}$$

where $\boldsymbol{f}_i(t)$ is a Gaussian, Markov stochastic function with zero mean and satisfies

$$\langle\boldsymbol{f}_i(t)\boldsymbol{f}_j(t')\rangle = 2D_S^S(\phi)\delta(t - t')\delta_{ij}\mathbf{1}. \tag{19}$$

Here the short-time self-diffusion coefficient D_S^S is given by

$$D_S^S(\phi) = \frac{D_0}{1 + L(\phi)}. \tag{20}$$

Equation (18) is a starting equation to solve numerically by BD simulations if D_S^S is known. Then, the long-time self-diffusion coefficient D_S^L is described by Eq. (2).

III. FIRST-PRINCIPLES EXPRESSION FOR D_S^L

In this section, we briefly discuss the first-principles derivation of the long-time self-diffusion coefficient D_S^L both in suspensions (S) and in molecular systems (M).

In order to obtain $D_S^L(\phi)$, it is convenient to introduce the mean-square displacement by

$$M_2(t) = \langle|\boldsymbol{X}_i(t) - \boldsymbol{X}_i(0)|^2\rangle. \tag{21}$$

Then the long-time self-diffusion coefficient D_S^L is given by

$$D_S^L(\phi) = \lim_{t\to\infty} \frac{M_2(t)}{6t}. \tag{22}$$

The starting equation is given by Eq. (5) for suspensions, on a time scale of order t_B, while it is given by the Newton equation for molecular systems, on a time scale of order t_0,

$$\frac{d}{dt}\boldsymbol{P}_i(t) = \boldsymbol{F}_i(t), \tag{23}$$

where $\boldsymbol{F}_i$ is given by Eq. (12) and $t_0 = \sigma/v_{th}$, v_{th} [$= (k_BT/m)^{1/2}$] being a thermal velocity. As shown in previous papers [32–34], on the time scale of order t_i, $M_2(t)$ then obeys

$$\frac{d}{dt}M_2(t) = 6D(t) \tag{24}$$

with the time-dependent self-diffusion coefficient

$$\frac{D(t)}{\Delta_0} = \begin{cases} \frac{D_S^S/D_0}{1+\frac{D_S^S}{D_0}\int_0^t \psi_S(s)ds} & \text{for } (S), \\ \frac{1}{t^{-1}+\int_0^t \psi_M(s)ds} & \text{for } (M), \end{cases} \tag{25}$$

where $\Delta_0 = D_0$ for (S), and $\Delta_0 = \sigma v_{th}$ for (M). Here the function $\psi_i(t)$ indicates the memory function, which is given by the correlation function of the fluctuating force. Use of Eq. (22) thus leads to

$$\frac{D_S^L}{\Delta_0} = \begin{cases} \frac{D_S^S/D_0}{1+\frac{D_S^S}{D_0}\int_0^\infty \psi_S(s)ds} & \text{for } (S), \\ \frac{1}{\int_0^\infty \psi_M(s)ds} & \text{for } (M). \end{cases} \tag{26}$$

In (S) there are three kinds of interaction acting on colloids. The first is a force exerted by the fluctuating fluid on colloids. The second is the hydrodynamic interactions between colloids. The last is the interactions between colloids through the potential $U_n(r)$. Hence the memory function $\psi_S(t)$ consists of the following three types of many-body correlation [32]:

$$\psi_S(t) = \psi_S^{FF}(t) + \psi_S^{FH}(t) + \psi_S^{HH}(t) \tag{27}$$

with the force term

$$\psi_S^{FF}(t) = \frac{\langle \boldsymbol{F}_i(t)\cdot\boldsymbol{F}_i(0)\rangle + \int_0^t \psi_S(s)ds\langle \boldsymbol{P}_i(t)\cdot\boldsymbol{F}_i(0)\rangle}{\langle \boldsymbol{P}_i(t)\cdot\boldsymbol{P}_i(0)\rangle}, \tag{28}$$

the hydrodynamic term

$$\psi_S^{HH}(t) = \frac{\langle \boldsymbol{H}_i(t)\cdot\boldsymbol{H}_i(0)\rangle + \int_0^t \psi_S(s)ds\langle \boldsymbol{P}_i(t)\cdot\boldsymbol{H}_i(0)\rangle}{\langle \boldsymbol{P}_i(t)\cdot\boldsymbol{P}_i(0)\rangle}, \tag{29}$$

and the coupling term

$$\psi_S^{HF}(t) = \frac{\langle \boldsymbol{H}_i(t)\cdot\boldsymbol{F}_i(0)\rangle + \langle \boldsymbol{F}_i(t)\cdot\boldsymbol{H}_i(0)\rangle}{\langle \boldsymbol{P}_i(t)\cdot\boldsymbol{P}_i(0)\rangle}. \tag{30}$$

On the other hand, in (M) there is only one interaction acting on molecules through the potential $U_n(r)$. Hence $\psi_M(t)$ consists of the force-force correlation $\psi_M{}^{FF}(t)$ only [33]. When the long-time hydrodynamic interactions are neglected, the memory functions $\psi_i(t)$ in both systems (S) and (M) thus coincide with each other. In the present paper, we discuss the dynamics of colloids and molecules only in a liquid state. Then, only the two-body correlation may play a role in $\psi_i(t)$, leading to

$$\psi_i(t) \simeq \frac{\langle \boldsymbol{F}_i(t)\cdot\boldsymbol{F}_i(0)\rangle}{\langle \boldsymbol{P}_i(t)\cdot\boldsymbol{P}_i(0)\rangle} + O(F^3). \tag{31}$$

By comparing Eq. (26) with Eq. (2) in (S), one thus finds

$$\int_0^\infty \psi_i(s)ds = \kappa\frac{x}{(1-x)^2}, \tag{32}$$

where $x = \phi/\phi_c$. Thus, it turns out that near the singular point ϕ_c, the long-time self-diffusion coefficient D_S^L/D_0 in (S) coincides with $D_S^L/\sigma v_{th}$ in (M), leading to

$$D_S^L/\Delta_0 \simeq \kappa^{-1}(1-x)^2. \tag{33}$$

In general, the analytic form of the short-time self-diffusion coefficient D_S^S is not known, except in hard-sphere suspensions [11]. Hence we next discuss how to obtain it numerically by performing two types of simulations, BD and MD. First, we use the fact that near ϕ_c the long-time self-diffusion coefficients obtained by the BD and MD simulations are described by Eq. (33). Second, we use the fact that if one scales time t by $(D_S^S/D_0)t$ in Eq. (18), the resulting equation is identical to Eq. (18) with $D_S^S = D_0$. This is the usual case where BD simulations are performed without the hydrodynamic interactions. As shown in the previous paper [14], D_S^L obtained by BD simulation without the hydrodynamic interactions is then described by

$$\frac{D_S^L(\phi)}{D_0} = \frac{1}{1+\kappa\frac{D_S^S(\phi)}{D_0}\frac{x}{(1-x)^2}}. \tag{34}$$

Near ϕ_c, we thus obtain

$$\frac{D_S^L(\phi)}{D_0} \simeq \frac{D_0}{D_S^S(\phi)}\kappa^{-1}(1-x)^2. \tag{35}$$

If one multiplies Eq. (34) by (D_S^S/D_0) later, therefore, it reduces to Eq. (2). Conversely, one can find D_S^S/D_0 by dividing Eq. (33) in (M) by Eq. (35) in (S). Hence two types of simulation, MD simulations and BD simulations without the hydrodynamic interactions, must be done separately. Thus, D_S^S/D_0 is obtained numerically by dividing the MD results by the BD results.

IV. HYDRODYNAMIC INTERACTIONS IN HARD-SPHERE SUSPENSIONS

By considering hard-sphere suspensions, we now discuss the two types of hydrodynamic effect on the self-diffusion coefficients, the short- and the long-time effects. For hard spheres, one finds $\kappa = 1.0$ from Eq. (3) since $n = \infty$.

As shown in a previous paper [11], for a suspension of hard spheres, the short-time hydrodynamic effect $L(\phi)$ is analytically calculated as

$$L(\phi) = \frac{2B^2}{1-B} - \frac{C}{1+2C} - \frac{BC(2+C)}{(1+C)(1-B+C)}, \tag{36}$$

where $B = (9\phi/8)^{1/2}$ and $C = 11\phi/16$. Then, the short-time self-diffusion coefficient given by Eq. (20) agrees well with the experimental data obtained by van Megen *et al.* [2,6]. As

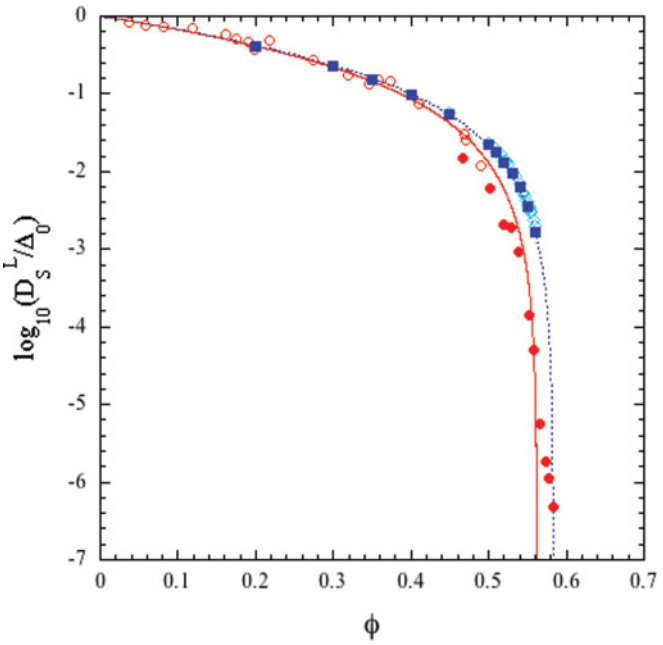

FIG. 1. (Color online) A logarithmic plot of the long-time self-diffusion coefficient D_S^L/Δ_0 versus ϕ for the experimental data and the simulation results. The filled squares indicate the BD results on hard spheres with 6% size polydispersity [14] and the open diamonds the MD results on hard spheres with 6% size polydispersity [35]. The filled circles indicate the experimental data from Ref. [6] and the open circles from Ref. [2]. The dotted line indicates the theoretical result given by Eq. (2) at $\phi_c \simeq 0.586$ and the solid line at $\phi_c \simeq 0.562$, where $\kappa = 1.0$.

discussed in a previous paper [14], the short-time self-diffusion coefficient obtained by dividing the MD results by the BD results without the hydrodynamic interactions also agrees with Eq. (36).

We next discuss the long-time hydrodynamic effects by comparing the MD and the BD simulation results on hard spheres with 6% size polydispersity [14] with the experimental data [2,6] obtained for colloidal hard spheres with 6% size polydispersity. In MD the force acting on the particle of interest is due to only the direct interactions between particles, while in BD it is due to both the direct interactions and the short-time hydrodynamic interactions. On the other hand, in experiments not only the direct interactions and the short-time hydrodynamic interactions but also the long-time hydrodynamic interactions play an important role in diffusion. In Fig. 1, the long-time self-diffusion coefficient D_S^L/Δ_0 for experiments and simulations is plotted versus ϕ. Here we note that since the original BD simulations [14] were performed under $D_S^S = D_0$ without hydrodynamic interactions, we have multiplied those results by D_S^S and used Eq. (36) in Fig. 1. Then, the BD results perfectly coincide with the MD results, where both results are well described by Eq. (2) with $\kappa = 1.0$ and $\phi_c = 0.586$. This means that the singular point $\phi_c \simeq 0.586$ for both simulations is determined only by the two-body correlations due to the direct interactions between hard spheres [14]. On the other hand, the singular point for the experiments is $\phi_c \simeq 0.562$. Thus, the difference between experiments and simulations may be caused by the long-time hydrodynamic interactions given by $\psi_S^{HH}(t)$ and $\psi_S^{FH}(t)$, although there are other possibilities, such as the intrinsic uncertainties in the experimental determination of the volume fraction. We should also note here that in both simulations crystallization occurs at $\phi \simeq 0.560$, while in the experiments the glass transition occurs at $\phi \simeq 0.5604$ where the experimental data start to deviate from the singular function at $\log_{10}(D_S^L/D_0) = -5.1$, leading to a nonequilibrium glass state [30,31]. This difference is also caused by the long-time hydrodynamic interactions. Thus, the hydrodynamic interactions are necessary to cause the glass transition for a suspension of hard spheres with 6% size polydispersity. Since all the results are described by the same singular function given by Eq. (2), except ϕ_c, they all must collapse on a single curve if they are plotted versus ϕ/ϕ_c. In fact, this is shown in Fig. 2.This situation is also expected for soft spheres.

V. ANALYSES OF EXPERIMENTAL DATA FOR BIOMOLECULES

We first analyze the experimental data for suspensions of biomolecules: hemoglobin and myoglobin measured by Doster and Longevin [19], lysozyme by Porcar *et al.* [20], α-crystallin by Giannoulou *et al.* [21], lecithin by Wolf and Kleinpeter [22], and myoglobin by Nesmelova and Fedetov [23]. As discussed in Ref. [30], those experimental data are well described by Eq. (2) with the hard-sphere values given by Eq. (36) at $\kappa = 2.0$, where the fitting values of singular point ϕ_c are listed in Table I. In Fig. 3, all data for D_S^L are plotted versus ϕ, where the theoretical line is given by Eq. (2) at $\kappa = 2.0$. In Fig. 4, all data are also plotted versus ϕ/ϕ_c. Thus, it is shown that within error, all data are collapsed onto a single line given by Eq. (2) with Eq. (36) at $\kappa = 2.0$ and $\phi_c = 0.558$. This suggests the following two important results. (i) The first is that $\kappa = 2.0$ leads to $n = 6$ from Eq. (3). (ii) The second

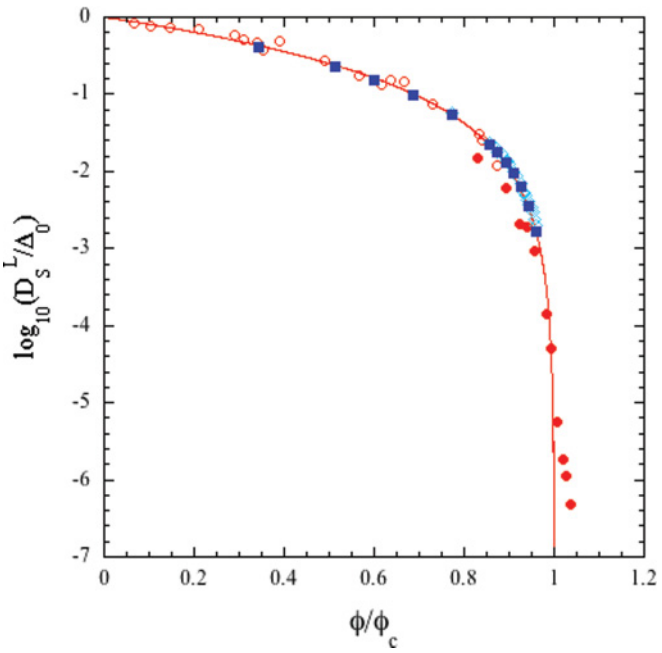

FIG. 2. (Color online) A logarithmic plot of the long-time self-diffusion coefficient D_S^L/Δ_0 versus ϕ/ϕ_c for the experimental data and the simulation results. The details are the same as in Fig. 1.

TABLE I. ϕ_c for different biomolecules at $\kappa = 2.0$, where W_0 is the water-asolectin weight ratio and PDADMAC the polydiallyldimethylammonium chloride.

System	ϕ_c	Symbol	Reference
Hemoglobin	0.495	$\odot$	[19]
Lysozyme	0.51	$+$	[20]
Myoglobin	0.560	$\times$	[19]
α-crystallin	0.590	$\diamond$	[21]
Lecithin ($W_0 = 0.080$)	0.600	$\triangledown$	[22]
Lecithin ($W_0 = 0.286$)	0.630	$\triangle$	[22]
Myoglobin	0.700	$\bullet$	[23]
Lecithin ($W_0 = 0.286$ PDADMAC)	0.710	$\triangleleft$	[22]
BD for modified potential ($n = 6$)	1.09	$\square$	—

is that the short-time self-diffusion coefficient is identical to that obtained theoretically for hard spheres. Hence those biomolecules behave like hard spheres for a short time, but they behave like soft spheres for a long time because $\kappa = 2.0$. For comparison, the theoretical line for hard spheres at $\kappa = 1.0$ is also plotted in Fig. 4, where $\phi_c = 0.558$. The experimental data for biomolecules are all shown not to obey a theoretical line with $\kappa = 1.0$ for hard spheres. Thus, the soft-core potential must satisfy those two conditions to describe the experimental data qualitatively. Next we discuss this.

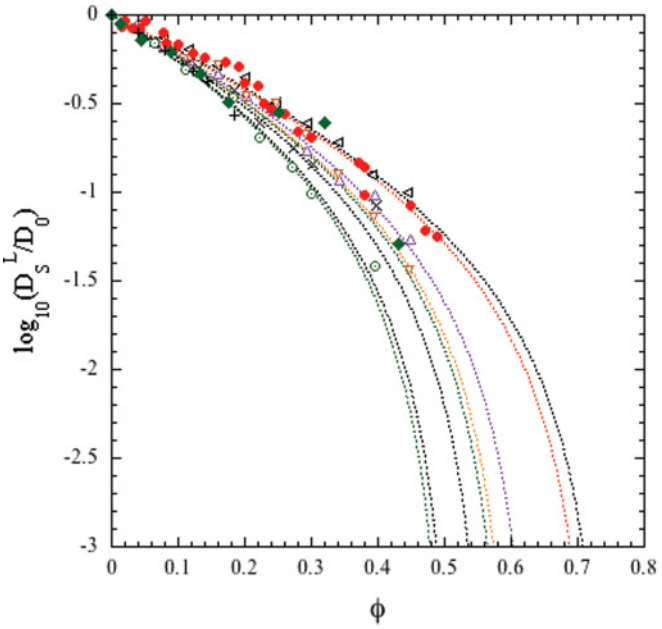

FIG. 3. (Color online) A logarithmic plot of the long-time self-diffusion coefficient D_S^L/D_0 versus ϕ for the experimental data and the simulation results. The symbols indicate the experimental data and the simulation results: ($\circ$) myoglobin from [23], ($\diamond$) α-crystallin from [21], ($\times$) myoglobin from [19], ($\odot$) hemoglobin from [19], ($\triangledown$) lecithin at $W_0 = 0.080$ from [22], ($\triangle$) lecithin at $W_0 = 0.286$ from [22], ($\triangleleft$) lecithin at $W_0 = 0.286$ (PDADMAC) from [22], and ($+$) lysozyme from [20]. The dotted lines (from left to right) indicate the theoretical lines given by Eq. (2) with Eq. (36) for experimental data at each ϕ_c listed in Table I (from top to bottom), where $\kappa = 2.0$.

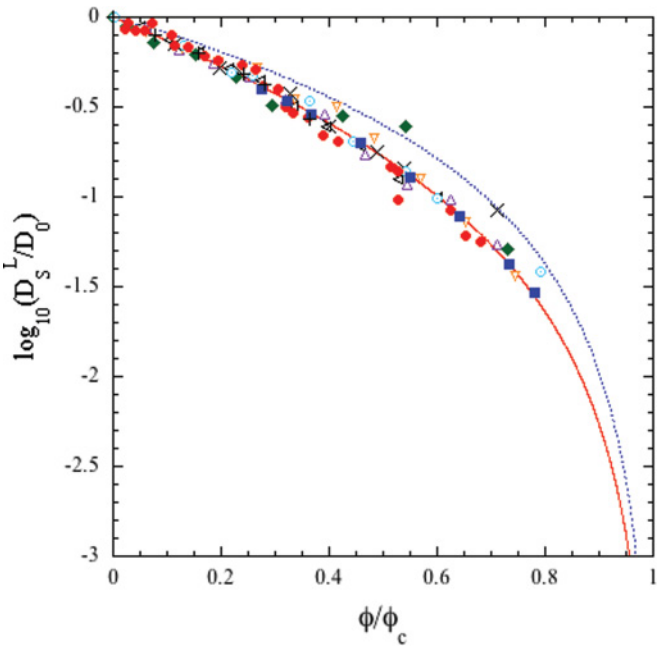

FIG. 4. (Color online) A logarithmic plot of the long-time self-diffusion coefficient D_S^L/D_0 versus ϕ/ϕ_c. The solid line indicates the theoretical line given by Eq. (2) with Eq. (36) at $\kappa = 2.0$ and $\phi_c = 0.558$ and the dotted line the theoretical line for hard spheres at $\kappa = 1.0$ and $\phi_c = 0.558$. The details are the same as in Fig. 3.

VI. BD AND MD SIMULATIONS FOR SOFT SPHERES

We now perform two types of simulation, BD simulations on suspensions of soft spheres and MD simulations on soft

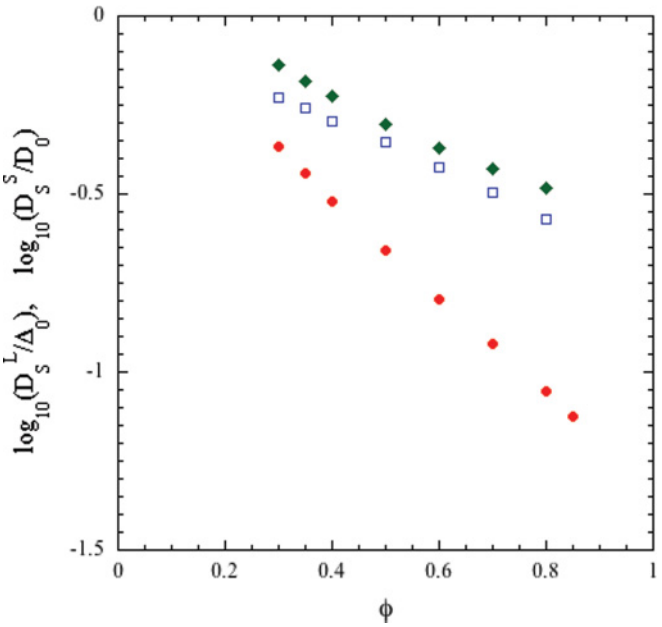

FIG. 5. (Color online) A logarithmic plot of the long-time self-diffusion coefficient D_S^L/Δ_0 versus ϕ for the BD and MD simulation results with the conventional soft-core potential at $b = 0$. The open squares indicate the BD results with $D_S^S = D_0$ and the filled circles the MD results. The filled diamonds indicate the short-time self-diffusion coefficient obtained by dividing the MD results by the BD results.

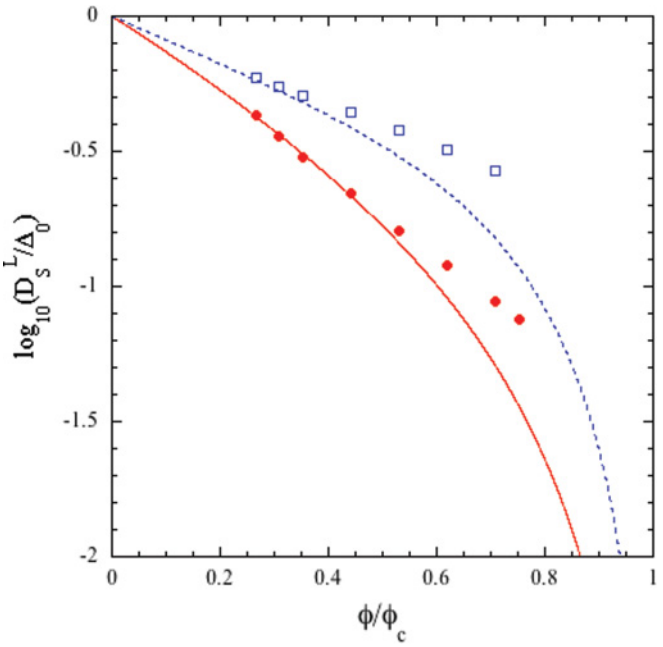

FIG. 6. (Color online) A logarithmic plot of the long-time self-diffusion coefficient D_S^L/Δ_0 versus ϕ for the BD and MD simulation results with the conventional soft-core potential at $b = 0$. The solid line indicates the theoretical result given by Eq. (2) with Eq. (36) and the dashed line that given by Eq. (34) with Eq. (36) at $\kappa = 2.0$ and $\phi_c = 0.558$. The details are the same as in Fig. 5.

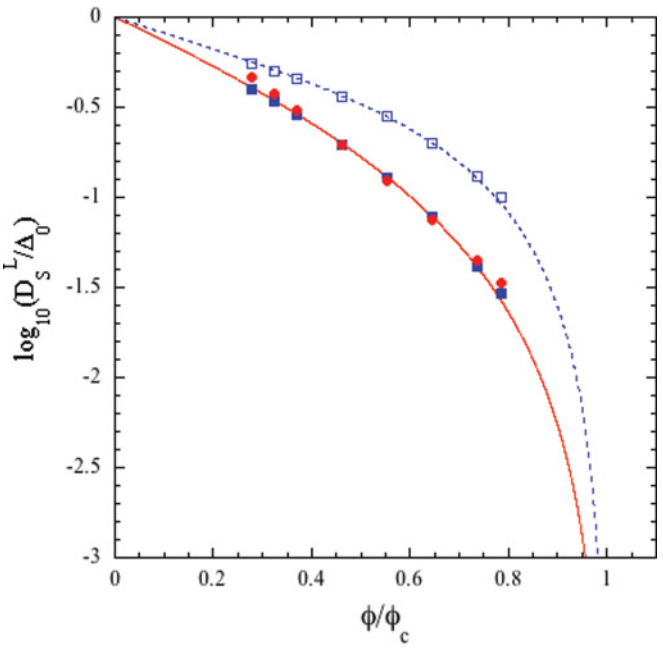

FIG. 7. (Color online) A logarithmic plot of the long-time self-diffusion coefficient D_S^L/Δ_0 versus ϕ for the BD and the MD simulation results with the modified soft-core potential at $b = 0.25$. The open squares indicate the BD results with $D_S^S = D_0$, the filled squares with D_S^S, and the filled circles the MD results. The solid line indicates the theoretical result given by Eq. (2) with Eq. (36) and the dashed line that given by Eq. (34) with Eq. (36) at $\phi_c \simeq 1.084$ and $\kappa = 2.0$.

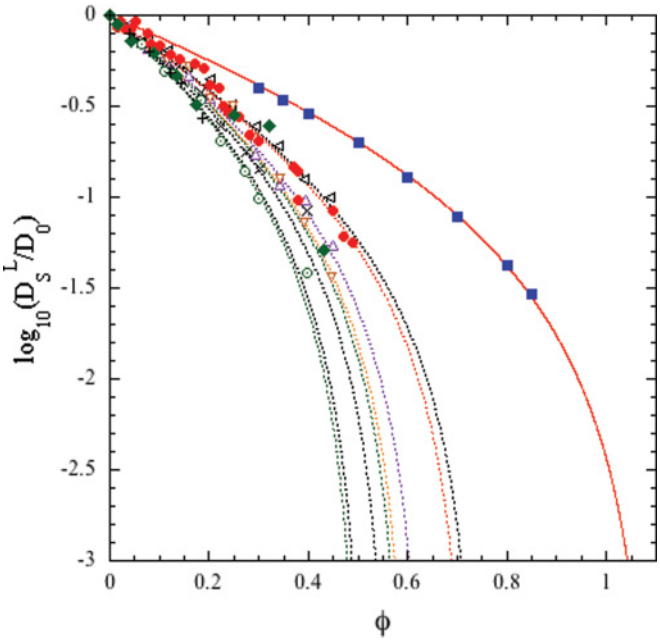

FIG. 8. (Color online) A logarithmic plot of the long-time self-diffusion coefficient D_S^L/D_0 versus ϕ. The details are the same as in Figs. 3 and 7.

spheres, under the conventional soft-core potential given by Eq. (1) and also the modified one given by Eq. (2) separately where $n = 6$, and $N = 10\,976$ for BD and 2048 for MD. By dividing the MD results by the BD results, we first obtain the short-time self-diffusion coefficient D_S^S numerically and then check whether it is identical to that obtained for hard spheres.

The starting equation for the MD simulations is given by Eq. (23). We scale space by σ, time by t_0 $(= \sigma/v_{th})$, and force by k_BT/σ. We employ the velocity Verlet method to integrate Eq. (23) with time step $10^{-3}t_0$ under periodic boundary and appropriate initial conditions. On the other hand, the starting equation for the BD simulation is given by Eq. (18). We also scale space by σ and time by t_D $(= \sigma^2/D_0)$. We employ the forward Euler difference scheme to integrate Eq. (18) with time step $10^{-4}t_D$ under periodic boundary and appropriate initial conditions. In both simulations, we start from a random configuration obtained by melting the fcc configuration and wait for a long time of order 10^4t_D (or 10^4t_0) which is enough to reach a final equilibrium state. In order to find the long-time self-diffusion coefficient, we use Eq. (22).

A. Conventional soft-core potential

We first discuss the simulations for the conventional potential given by Eq. (1), where $n = 6$. Here the effective diameter is $\sigma_{eff} = \sigma$. We set $D_S^S = D_0$ since the numerical values of D_S^S are not known for the conventional potential. In Fig. 5, the BD and the MD results are shown versus ϕ. The short-time self-diffusion coefficient, which is obtained by dividing the MD results by the BD results, is also plotted. In order to check whether those results satisfy the conditions (i) and (ii) discussed before, we also plot those results versus ϕ/ϕ_c in Fig. 6. Since the singular point ϕ_c for the simulation results is not known, we adjust it so that the BD results coincide well with the theoretical line. Then we find $\phi_c \simeq 1.13$ for both

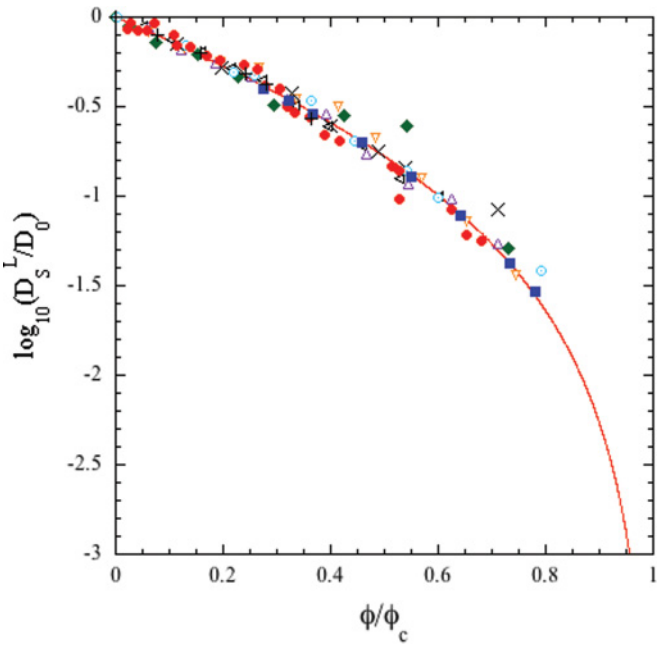

FIG. 9. (Color online) A logarithmic plot of the long-time self-diffusion coefficient D_S^L/D_0 versus ϕ/ϕ_c. The details are the same as in Figs. 4 and 7.

results. The solid line in Fig. 6 is the same as that in Fig. 4. Thus, we conclude that the conventional soft-core potential does not describe the long-time self-diffusion for biomolecules at all.

B. Modified soft-core potential

We next discuss the simulations for the modified potential given by Eq. (4), where $n = 6$. Here the effective diameter is $\sigma_{eff} = (1 + b)\sigma$. In BD, Eq. (20) with Eq. (36) is used to solve Eq. (18). The unknown parameter b is chosen so that the BD results coincide with the MD results. The several simulation results suggest $b \simeq 0.25$. In Fig. 7, both simulation results are plotted versus ϕ. For comparison, the BD simulation results with $D_S^S = D_0$ are also shown. Both results are well described by the theoretical lines given by Eq. (2) with Eq. (36) and Eq. (34) with Eq. (36) at $\kappa = 2.0$ and $\phi_c = 1.09$, where ϕ in both equations is replaced by $\phi/(1 + b)^3$. Thus, the modified potential can qualitatively describe the self-diffusion of biomolecules well. In Fig. 8, the BD results with D_S^S are plotted versus ϕ together with the experimental data. As shown in Table I, the singular point of the simulations is much larger than that of the experiments. There are several reasons for this. One of the main reasons is because we do not consider the long-time hydrodynamic interactions in the simulations at all. Those interactions reduce the singular point to a lower value. This situation is the same as that in Fig. 1. Another reason may be because we choose the simplest form for $U_n(r)$. In all cases, the singular point strongly depends on the details of the system. If one scales ϕ by ϕ_c, however, this difference disappears. In fact, as is shown in Fig. 9, the BD results with D_S^S are collapsed onto the same singular curve as that on which the experimental data are all collapsed.

VII. SUMMARY

In the present paper, we have proposed the simple model potential given by Eq. (4) with $n = 6$ and $b = 0.25$ to describe self-diffusion of biomolecules. This form was suggested from the analyses of experimental data for soft spheres [30] indicating that soft spheres behave as hard spheres for short times while they behave as soft spheres with an exponent $n = 6$ for long times. Then, we performed not only extensive Brownian-dynamics simulations on monodisperse soft spheres with the modified soft-core potential but also those with the conventional one. Thus, we have shown that the soft spheres with the modified potential can be treated as hard spheres for short times, leading to D_S^S given by Eq. (20) with Eq. (36). We have also shown that the volume fraction dependence of their long-time self-diffusion coefficients is qualitatively in good agreement with that observed in the experiments, while the conventional results are not. We should note here that there still exists a quantitative difference between the experiments and the simulations with the modified potential since the singular point of the simulations is always larger than that of experiments. The singular point strongly depends on the details of the system. One of the main reasons is because the long-time hydrodynamic interactions are completely neglected in the simulations. In fact, they will reduce the singular point as seen in colloidal suspensions (see Fig. 1). However, it is still a difficult problem to solve Eq. (5) itself even numerically because of the long-range nature of the hydrodynamic interaction tensor $\boldsymbol{g}_{ij}$. Another reason might be because the charge effects (i.e., attractive interactions) [36], the deformation of spheres, and so on are not considered. In any case, the proposed potential must satisfy two conditions consistently, (i) $\kappa = 2.0$ (or $n = 6$) and (ii) D_S^S is identical to that obtained for hard spheres. This will be discussed elsewhere.

ACKNOWLEDGMENTS

We thank the referees for helpful comments. This work was partially supported by World Premier International Research Center Initiative, MEXT, Japan and also by Institute of Fluid Science, Tohoku University. The simulations were performed using the SGI Altix3700Bx2 in Advanced Fluid Information Research Center, Institute of Fluid Science, Tohoku University.

[1] P. N. Pusey and W. van Megen, Nature (London) **320**, 340 (1986).
[2] W. van Megen and S. M. Underwood, J. Chem. Phys. **91**, 552 (1989).
[3] R. H. Orttewill and N. St. J. Williams, Nature (London) **325**, 232 (1987).
[4] P. N. Pusey, in *Liquids, Freezing and the Glass Transition*, edited by J. P. Hansen, D. Levesque, and J. Zinn-Justin (Elsevier, Amsterdam, 1991).
[5] A. van Blaaderen, J. Peetermans, G. Maret, and K. J. G. Dhont, J. Chem. Phys. **96**, 4591 (1992).

[6] W. van Megen, T. C. Mortensen, S. R. Williams, and J. Müller, Phys. Rev. E **58**, 6073 (1998).
[7] P. Mazur, Physica A **110**, 181 (1982).
[8] C. W. Beenakker and P. Mazur, Physica A **120**, 388 (1983).
[9] M. Medina-Noyola, Phys. Rev. Lett. **60**, 2705 (1988).
[10] J. A. Leegwater and G. Szamel, Phys. Rev. A **46**, 4999 (1992).
[11] M. Tokuyama and I. Oppenheim, Phys. Rev. E **50**, R16 (1994).
[12] M. Tokuyama and I. Oppenheim, Physica A **216**, 85 (1995).
[13] B. Cichoki and K. Hinsen, Physica A **166**, 437 (1990).
[14] M. Tokuyama, H. Yamazaki, and Y. Terada, Phys. Rev. E **67**, 062403 (2003); Physica A **328**, 367 (2003).
[15] A. George and W. W. Wilson, Acta Crystallogr. Sect. D **50**, 361 (1994).
[16] O. D. Velve, E. W. Kaler, and A. M. Lenhoff, Biophys. J. **75**, 2682 (1998).
[17] B. Lonetti, E. Fratini, S. H. Chen, and P. Baglioni, Phys. Chem. Chem. Phys. **6**, 1388 (2004).
[18] A. Strander, H. Sedgwick, F. Cardinaux, W. C. K. Poon, S. U. Egelhaaf, and P. Schurtenberger, Nature (London) **432**, 492 (2004).
[19] W. Doster and S. Longeville, Biophys. J. **93**, 1360 (2007).
[20] L. Porcar, P. Falus, W-R. Chen, A. Faraone, E. Fratini, K. Hong, P. Baglioni, and Y. Liu, J. Phys. Chem. Lett. **1**, 126 (2010).
[21] A. Giannopoulou, A. J. Aletras, N. Pharmakakis, G. N. Papatheodorou, and S. N. Yannopoulos, J. Chem. Phys. **127**, 205101 (2007).
[22] G. Wolf and E. Kleinpeter, Langmuir **21**, 6742 (2005).
[23] I. V. Nesmelova and V. D. Fedotov, BioChim. Biophys. Acta **1383**, 311 (1998).
[24] A. P. Minton, J. Biol. Chem. **276**, 10577 (2001); **127**, 205101 (2007).
[25] C. Le Coeur and S. Longeville, Chem. Phys. **345**, 298 (2008).
[26] P. Mereghetti, R. R. Gabdoulline, and R. C. Wade, Biophys. J. **99**, 3782 (2010).
[27] S. Barhoum and A. Yethiraj, J. Phys. Chem. B **114**, 17062 (2010).
[28] M. Tokuyama, Physica A **364**, 23 (2006).
[29] M. Tokuyama, Phys. Rev. E **80**, 031503 (2009).
[30] M. Tokuyama, J. Non-Cryst. Solids **357**, 293 (2011).
[31] M. Tokuyama, Phys. Rev. E **82**, 041501 (2010).
[32] M. Tokuyama, Physica A **387**, 4015 (2008); **387**, 5675 (2008).
[33] M. Tokuyama, Physica A **387**, 5003 (2008).
[34] M. Tokuyama, Physica A **389**, 951 (2010).
[35] M. Tokuyama and Y. Terada, J. Phys. Chem. B **109**, 21357 (2005).
[36] M. Broccio, D. Costa, Y. Liu, and S.-H. Chen, J. Chem. Phys. **124**, 084501 (2006).